The solid- and solution-state structures of 2-nitrosopyridine and its 3- and 4-methyl derivatives

Brian G. Gowenlock,[a] Mark J. Maidment,[a] Keith G. Orrell,*[a] Vladimir Šik,[a] Giuseppe Mele,[b] Giuseppe Vasapollo,[b] Michael B. Hursthouse[c] and K. M. Abdul Malik[d]

[a] *School of Chemistry, The University, Exeter, UK EX4 4QD. E-mail: K.G.Orrell@exeter.ac.uk*
[b] *Dipartimento di Ingegneria dell'Innovazione, Università di Lecce, Via Arnesano, 73100 Lecce, Italy*
[c] *Department of Chemistry, University of Southampton, Southampton, UK SO17 1BJ*
[d] *Department of Chemistry, University of Wales Cardiff, PO Box 912, Cardiff, UK CF1 3TB*

Received (in Cambridge, UK) 30th May 2000, Accepted 5th September 2000
First published as an Advance Article on the web 19th October 2000

2-Nitrosopyridine, **1**, 3-methyl-2-nitrosopyridine, **2**, and 4-methyl-2-nitrosopyridine, **3**, exist in organic solvents as monomer–azodioxy dimer equilibria with the dimers predominating at ambient temperatures. In the case of compounds **1** and **3** only the *Z*-dimers co-exist with the monomers, whereas for compound **2** both *Z*- (major) and *E*- (minor) dimers are present with the monomer. Variable temperature ^{1}H NMR bandshape analysis and 2D-EXSY spectra of **1**–**3** provided thermodynamic and kinetic data for the dissociation equilibria *Z*- (or *E*-) dimer $\rightleftharpoons$ 2 monomer, $\Delta H^{\ominus}$ values being in the range 53–58 kJ mol^{-1} and $\Delta G^{\ddagger}$ (298.15 K) values in the range 70–82 kJ mol^{-1}. An X-ray crystal structure of **1** identified the compound as a *Z*-dimeric species with the two pyridine rings twisted by 62.7° and their heterocyclic N atoms pointing towards each other.

In 1982 Taylor *et al.*[1] pointed out that only a few hetero-aromatic *C*-nitroso compounds were known and stated that this was in marked contrast to aromatic *C*-nitroso compounds. Stable dimers of 2-nitrosopyridine and 4-methyl-2-nitroso-pyridine were prepared,[1] both of which, when dissolved in organic solvents, dissociated to give typical blue solutions of monomeric *C*-nitroso compounds. Structural studies of these nitroso compounds were not however initiated and the isomeric character of the dimer was not established, neither were any quantitative studies of the dissociation equilibrium $(RNO)_2 \rightleftharpoons 2RNO$ performed. In a later paper[2] dimeric 3-methyl-2-nitrosopyridine was prepared and depicted as a *Z*-dimer although the authors did not provide any supporting evidence for this isomeric form.

Relatively few *C*-nitroso derivatives of six-membered hetero-aromatic systems have been prepared although there are two examples where crystallographic studies have identified the dimeric form, namely for tetrafluoro-4-nitrosopyridine[3,4] (*E*-dimer) and 2-nitrosoquinoxaline[5] (*Z*-dimer). There are, however, many examples of 3,5-disubstituted- and 1,3,5-trisubstituted-4-nitrosopyrazoles. These occur exclusively in the monomeric form[6,7] and may be compared with 4-nitroso-anilines. The successful syntheses of nitrosopyridines[1,2] now afford the opportunity to carry out detailed quantitative studies on these compounds which can be compared with those for the corresponding nitrosobenzenes. This paper describes such studies on 2-nitrosopyridine and its 3- and 4-methyl derivatives, using NMR methods for the solution investigations, and IR spectroscopy and X-ray crystallography for solid state investigations.

Experimental

Preparations of compounds

The general method of preparing the 2-nitrosopyridines involved reacting the appropriate 2-aminopyridine with dimethyl sulfide and *N*-chlorosuccinimide, deprotonating the resulting sulfonium salts with sodium methoxide to the *S*,*S*-dimethylsulfilimines and oxidising with *m*-chloroperbenzoic acid. This route was previously reported by Taylor *et al.* for 2-nitrosopyridine,[1] 3-methyl-2-nitrosopyridine,[2] and 4-methyl-2-nitrosopyridine.[1] The compounds **1**, **2** and **3** were tan

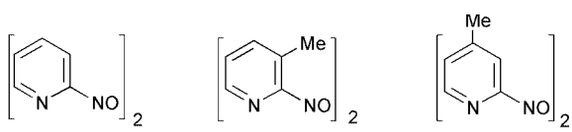

1 **2** **3**

coloured solids, which dissolved readily in organic solvents to give pale green solutions.

Spectroscopic methods

Infrared spectra were recorded on **1**, **2** and **3** as KBr discs using Nicolet Magna or Avatar 360 FT spectrometers.

NMR spectra were recorded on solutions of **1**, **2** and **3** in $CDCl_3$ (for ambient temperature studies) and $(CDCl_2)_2$ (for high temperature studies) using a Bruker Avance DRX 400 spectrometer operating at 400 MHz for ^{1}H spectra. Additional solvents (see text) were also used to study compound **2**. Probe temperatures were varied using a Bruker B-VT-2000 unit and care was taken to ensure good temperature stability before any spectra were recorded. NMR bandshapes were analysed using the authors' version of the original DNMR3 program.[8] The computer simulated spectra were compared visually with those obtained experimentally and the 'best-fit' rate constants, measured over as wide a temperature range as possible, were used to calculate the activation parameters from least squares fittings of standard Eyring plots. The errors quoted are based on the goodness-of-fit of such plots. Kinetic data for the *Z*- and *E*-dimer dissociations of **2** were measured by two-dimensional exchange spectroscopy (2D-EXSY) NMR experiments using the authors' D2DNMR program.[9] Signal intensities were measured by volume integrations. Mixing times used in the NOESYPH pulse sequence were in the range 0.2 to 1.0 s.

 DOI: 10.1039/b004270f

Table 1 Major IR bands of the dimeric azodioxy-2-nitrosopyridines **1**, **2** and **3**

$\tilde{\nu}$/cm^{-1} [a]			
1	**2**	**3**	Assignment
1593	1598	1606	
1565	1568	1559	
1465	1463sh	1477	
	1450		
1436			
1404 } vs, br	1389 vs, br	1383 vs, br	ω_{as} (*Z*-ONNO)
1386 }			ω_{s} (*Z*-ONNO)
1299	1289	1285	
1256	1257*	1251	*ω_{as} (*E*-ONNO)
1224	1221	1178	
1203	1116	1153	
1094			
994		996	
964 vs	956 vs	871, 857	δ (CNN)
796 } vs	809 vs	828 vs	
782 }			
691	661	696	

[a] vs, very strong; br, broad.

X-Ray crystallography

Crystal structure of the *Z*-azodioxy dimer of 2-nitrosopyridine. Pale tan crystals (size 0.2 × 0.3 × 0.2 mm) were obtained as described above and examined in Lindemann capillaries.

Crystal data. $C_{10}H_8N_4O_2$. $M = 216.20$, triclinic, space group $P\bar{1}$, $a = 6.231(2)$, $b = 8.198(3)$, $c = 10.300(4)$ Å, $\alpha = 99.17(3)°$, $\beta = 95.29(4)°$, $\gamma = 106.630(16)°$, $Z = 2$, $\mu = 0.107$ mm^{-1}.

Data collection and processing. Data were collected on an Enraf Nonius FAST TV area detector diffractometer mounted at the window of a rotating anode generator with a molybdenum anode as described elsewhere.[10] A total of 2035 reflections were collected in the theta range 2.02 to 25.03° resulting in 1351 independent reflections [R(int) = 0.2015].

Solution and refinement. The structure was solved by direct methods[11] and refined by full matrix least squares.[12] The final R_1 and ωR_2 values for data with $I > 2\sigma(I)$ were 0.0604 and 0.1203 respectively.

Additional material (atomic coordinates and anisotropic displacement parameters) has been deposited at the Cambridge Crystallographic Data Centre.†

Results

IR Spectra

The *C*-nitroso compounds **1**–**3** were tan coloured solids, indicative of dimeric species.[13] IR spectroscopy has been much used for characterising azodioxy dimers following early work by Lüttke.[14,15] Accordingly, IR spectra of the solids **1**–**3** were recorded as pressed KBr discs and the major bands listed in Table 1. Spectra in the region 1600–1200 cm^{-1} are relatively similar, but they differ significantly in the range 1200–800 cm^{-1}. Strong evidence for *Z*-dimeric species was obtained from the intense bands at 1404, 1386 (**1**), 1389 (**2**) and 1383 cm^{-1} (**3**), which, following earlier studies,[15,16] are associated with the antisymmetric and symmetric stretching modes of the *Z*-ONNO moiety. A strong unsplit band in the range 1250–1300 cm^{-1} is expected for the antisymmetric stretch of an *E*-ONNO moiety.[15,17] In the case of **2**, a moderately intense band at 1257 cm^{-1} was tentatively attributed to a small amount of this solid-state dimeric form. Such an attribution would account for the presence of a small amount of the *E*-azodioxy form of **2** in a range of organic solvents ($CDCl_3$, $(CDCl_2)_2$, CD_2Cl_2, $(CD_3)_2CO$ and $(CD_3)_2SO$). Other diagnostic bands are the C–N stretches, which are more correctly described as CNN deformations due to coupling effects. The intense bands at 964 (**1**), 956 (**2**) and 871, 857 cm^{-1} (**3**) are tentatively attributed to this mode, while the other bands are assigned to internal stretchings and deformation modes of the pyridyl rings.

† CCDC reference number 188/272. See http://www.rsc.org/suppdata/p2/b0/b004270f/ for crystallographic files in .cif format.

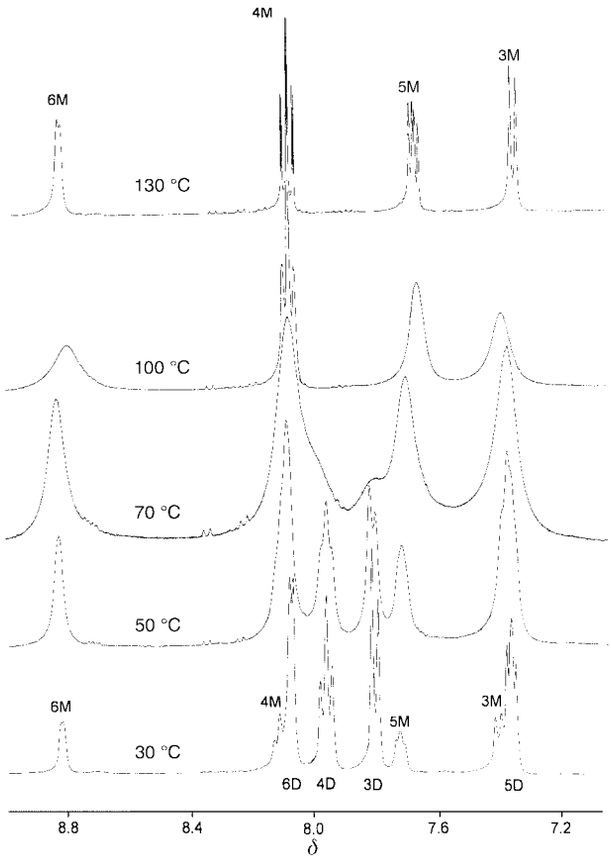

Fig. 1 Variable temperature ^{1}H NMR spectra of 2-nitrosopyridine, **1**, in $(CDCl_2)_2$ solution, showing the temperature effects of the monomer–dimer equilibrium.

NMR Spectra

2-Nitrosopyridine, 1. The room temperature ^{1}H spectra of **1** comprised eight multiplets which divided into a major and minor set (rel. intensity ~ 3.5 : 1), Fig. 1. On cooling a CD_2Cl_2 solution of **1**, the minor signals diminished in intensity and were virtually undetectable below *ca.* −50 °C. As solution equilibria of aromatic *C*-nitroso compounds invariably favour dimeric species on cooling, the major set of signals in the room temperature spectrum was attributed to a dimeric species. Thus, there appears to be a remarkably low degree of dissociation of the azodioxy dimer of **1** at ambient temperatures in contrast to most aromatic *C*-nitroso compounds, *e.g.* nitrosobenzene, which are fully dissociated at ambient temperatures in organic solvents. Assignments of the signals were straightforward and are shown in Fig. 1 and shifts listed in Table 2. These assignments were confirmed on warming a $(CDCl_2)_2$ solution of **1** up to 130 °C. This increased the rate of dissociation and produced exchange broadening between the pairs of monomer and dimer signals of the 3-, 4-, 5- and 6-position pyridyl hydrogens. This led to very broad, ill-defined spectra in the intermediate temperature range 60–100 °C, where appreciable amounts of monomeric and dimeric species co-exist. Above ~100 °C the spectral lines sharpened as exchange became fast on the NMR timescale and the monomeric species began to dominate, and by 130 °C dissociation was virtually complete as evidenced by a single set of sharp monomer signals. By integration of selected signals, carefully allowing for band overlaps and for the fact

that the dimer signals were due to pairs of hydrogens as opposed to single hydrogens in the case of the monomer signals, relative populations of both species were calculated in the temperature range 303–353 K. Relative populations at temperatures in the range 363–393 K were based on a linear extrapolation of the lower temperature data. These relative populations were expressed as $K^{\ominus}$ values (Table 3) for the dissociation equilibrium $D(Z) \rightleftharpoons 2M$ where $K^{\ominus} = [M]^2/[D]c^{\ominus}$ ($c^{\ominus} = 1$ mol dm^{-3}) (Scheme 1). A graph of ln $K^{\ominus}$ *versus* T^{-1} produced a good linear fit from which $\Delta H^{\ominus}$, $\Delta S^{\ominus}$, and subsequently $\Delta G^{\ominus}$ (298.15 K) values were calculated (Table 4). The assumption that the dimeric species in solution was the *Z*-dimer, D(*Z*), is based on previous studies of a wide range of *C*-nitrosobenzenes.[18]

Knowing the thermodynamic data associated with the monomer–dimer equilibria of **1**, kinetic data for the dimer dissociation were sought by the total NMR bandshape method. This was not straightforward because of the extensive number of band overlaps in the spectra at the temperatures of interest. Only the 6-position monomer signal (at $\delta \sim 8.8$) remained clear of overlaps and this was chosen for bandshape analysis. Allowance was made for scalar coupling to the 5-position hydrogen ($J_{56} = 3.4$ Hz) and computer fittings performed at temperatures 303, 323, 333, 343 and 353 K using the DNMR3 program.[8] 'Best-fit' rate constants (k/s^{-1}) were found to be 5, 43, 110, 280 and 685 respectively, and these enabled the Eyring activation parameters $\Delta H^{\ddagger}$, $\Delta S^{\ddagger}$ and $\Delta G^{\ddagger}$ (298.15 K) to be evaluated (Table 4).

The X-ray crystal structure of **1** (Fig. 2) identified the compound as a *Z*-azodioxy dimeric species with a dihedral angle of 62.7° between the two ring planes and the heterocyclic N atoms pointing towards each other with the N(1)–N(4) non-bonded distance being 2.964 Å. Bond lengths and angles are listed in Table 5. The N=N, N=O and C–N distances of the azodioxy functionality were 1.325(4), 1.274(3)/1.260(4) and 1.444(5)/1.468(4) Å respectively. These are all very comparable to corresponding distances in other *Z*-azodioxy species, namely the *Z*-dimers of nitrosobenzene,[19] perfluoronitrosobenzene[20] and 2-nitrosoquinoxaline.[5] Similar invariancy applies to the N–N–O and N–N–C angles in these compounds. More discussion of these solid-state structures will be reserved for the Discussion.

4-Methyl-2-nitrosopyridine, 3. This compound exhibited similar solution behaviour to **1**. At room temperature in $(CDCl_2)_2$ solvent the *Z*-azodioxy species predominated, but on warming dissociation occurred and the monomer form

Table 2 ^{1}H NMR data for compounds **1**–**3** in $(CDCl_2)_2$ at 303 K

		δ (*J*/Hz)		
Compound	H-position	Monomer	*Z*-Dimer	*E*-Dimer
1	3	7.40 (7.9)	7.80 (7.8)	
	4	8.12 (7.8, 7.8)	7.96 (7.9, 7.9)	
	5	7.72 (7.8, 3.4)	7.36 (7.9, 4.1)	
	6	8.82 (3.4)	8.08 (4.1)	
2	3 (Me)	3.35	2.53	2.50
	4	8.11 (8.1)	7.65 (7.7)	7.82 (8.2)
	5	7.54 (8.1, 3.9)	7.19 (7.7, 4.2)	7.49 (8.2, 3.9)
	6	8.36 (3.9)	7.96 (4.2)	8.52 (3.9)
3	3	7.24	7.61	
	4 (Me)	2.55	2.48	
	5	7.52 (4.4)	7.15 (4.9)	
	6	8.65 (4.5)	7.92 (5.0)	

Table 3 Dissociation equilibrium constants for compound **1** in $(CDCl_2)_2$

T/K	$T^{-1}/10^{-3}$ K^{-1}	$K^{\ominus}$	ln$^{\ominus}$
303	3.30	0.208	−1.57
323	3.10	0.778	−0.251
333	3.00	1.43	0.358
343	2.92	2.51	0.920
353	2.83	4.41	1.48
363	2.75	9.08	2.21
373	2.68	18.9	2.94
383	2.61	39.7	3.68
393	2.54	48.0	3.87

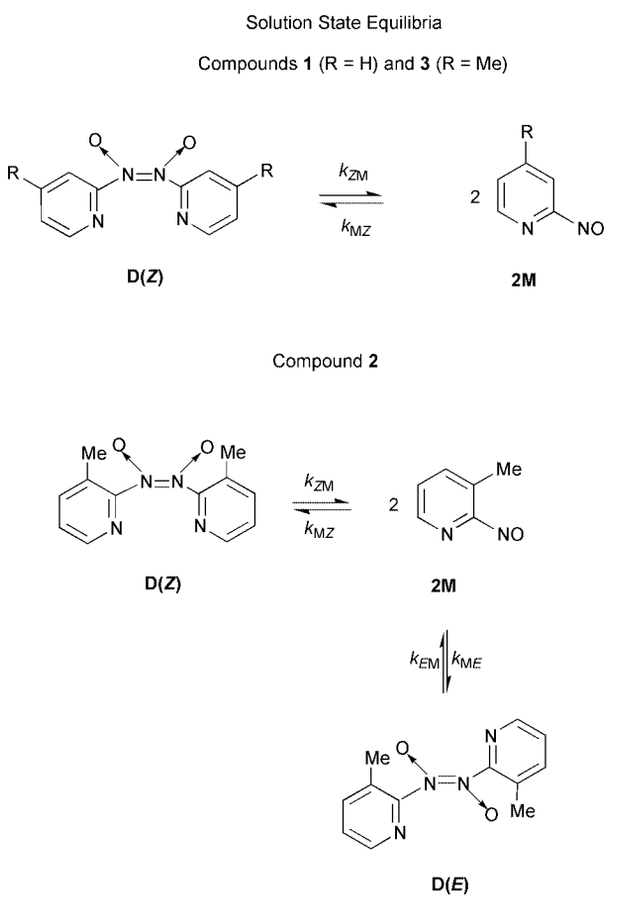

Scheme 1

Table 4 Thermodynamic and kinetic data for the dimer–monomer equilibria of compounds **1**–**3** in $(CDCl_2)_2$ solution

Compound	Equilibrium	$\Delta H^{\ominus}$/ kJ mol^{-1}	$\Delta S^{\ominus}$/ J K^{-1} mol^{-1}	$\Delta G^{\ominus}$ [a]/ kJ mol^{-1}	$\Delta H^{\ddagger}$/ kJ mol^{-1}	$\Delta S^{\ddagger}$/ J K^{-1} mol^{-1}	$\Delta G^{\ddagger}$ [a]/ kJ mol^{-1}
2-Nitrosopyridine **1**	$D(Z) \rightleftharpoons 2M$	54.0 ± 0.5	166 ± 1	4.6 ± 0.8	84.5 ± 0.4	47.3 ± 1.3	70.4 ± 0.1
3-Methyl-2-nitroso-pyridine **2**	$D(Z) \rightleftharpoons 2M$	58.4 ± 0.6	154 ± 2	12.5 ± 1.2	87.3 ± 10.1	17 ± 32	82.2 ± 0.5
	$D(E) \rightleftharpoons 2M$	—	—	−2.4 ± 0.1	88.5 ± 6.0	29 ± 19	79.8 ± 0.3
4-Methyl-2-nitroso-pyridine **3**	$D(Z) \rightleftharpoons 2M$	53.0 ± 0.9	163 ± 3	4.5 ± 0.8	94.2 ± 2.7	65 ± 8	74.8 ± 0.4
Nitrosobenzene [b]	$D(Z) \rightleftharpoons 2M$	55.5 ± 1.7	219 ± 7	−9.8 ± 0.3	88.5 ± 1.0	76 ± 3	65.8 ± 0.1
	$D(E) \rightleftharpoons 2M$	42.5 ± 1.2	185 ± 5	−12.6 ± 0.2	94.4 ± 4.4	82 ± 16	70.0 ± 0.3

[a] At 298.15 K. [b] Ref. 31.

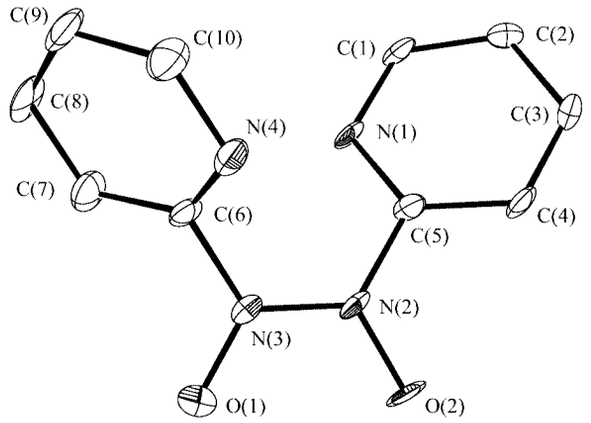

Fig. 2 Crystal structure of **1**, showing the *Z*-azodioxy dimeric form of the solid.

Table 5 Bond lengths (Å) and angles (°) for compound **1**

N(2)–O(2)	1.274(3)	N(2)–N(3)	1.325(4)
N(2)–C(5)	1.444(3)	N(3)–O(1)	1.260(4)
N(3)–C(6)	1.468(4)	N(1)–C(5)	1.323(4)
N(1)–C(1)	1.334(5)	N(4)–C(6)	1.299(4)
N(4)–C(10)	1.351(5)	C(5)–C(4)	1.371(5)
C(2)–C(1)	1.370(5)	C(2)–C(3)	1.376(5)
C(3)–C(4)	1.387(5)	C(10)–C(9)	1.365(6)
C(6)–C(7)	1.376(5)	C(8)–C(9)	1.362(6)
C(8)–C(7)	1.389(5)		
O(2)–N(2)–N(3)	118.1(3)	O(2)–N(2)–C(5)	119.0(3)
N(3)–N(2)–C(5)	122.5(2)	O(1)–N(3)–N(2)	119.6(2)
O(1)–N(3)–C(6)	119.0(3)	N(2)–N(3)–C(6)	120.4(3)
C(5)–N(1)–C(1)	115.4(3)	C(6)–N(4)–C(10)	114.7(3)
N(1)–C(5)–C(4)	126.0(3)	N(1)–C(5)–N(2)	116.1(3)
C(4)–C(5)–N(2)	117.9(3)	C(1)–C(2)–C(3)	118.6(4)
C(2)–C(3)–C(4)	118.9(3)	C(5)–C(4)–C(3)	116.9(3)
N(4)–C(10)–C(9)	123.6(4)	N(4)–C(6)–C(7)	127.6(3)
N(4)–C(6)–N(3)	115.3(3)	C(7)–C(6)–N(3)	117.0(3)
N(1)–C(1)–C(2)	124.2(3)	C(9)–C(8)–C(7)	119.3(4)
C(8)–C(9)–C(10)	119.2(4)	C(6)–C(7)–C(8)	115.5(4)

dominated at temperatures above ~60 °C. ^{1}H NMR spectra of both the aromatic and methyl hydrogens in the temperature range 30–130 °C are shown in Fig. 3. Dissociation equilibrium constants ($K^{\ominus}$), based on accurate integrations of suitable non-overlapping pairs of aromatic signals were measured for seven temperatures in the range 30–70 °C. These gave good linear van't Hoff plots from which $\Delta H^{\ominus}$, $\Delta S^{\ominus}$ and $\Delta G^{\ominus}$ values were calculated (Table 4).

Rates of *Z*-dimer dissociation were obtained by bandshape analysis of the 6-position hydrogen signals, measured at temperatures in the range 60–90 °C. These are shown in Fig. 4 together with the simulated bandshapes based on the 'best-fit' rate constants shown in this Figure. These rate constants provided the activation energy parameters listed in Table 4.

3-Methyl-2-nitrosopyridine 2. This methyl derivative differed from its 4-methyl counterpart by existing as both *Z*- and *E*-azodioxy dimers in equilibrium with the monomeric form in organic solvents. The *Z*-dimer population predominated at ambient and low temperatures, typical values (for $CDCl_3$ solvent, 323 K) being 74% (*Z*-dimer), 5% (*E*-dimer) and 21% (monomer). As previously, the monomer species dominated at above-ambient temperatures. Dissociation equilibrium constants $K^{\ominus}$ for the *Z*-dimers in $(CDCl_2)_2$ solvent were calculated by accurate integrations of non-overlapping signals in the temperature range 303–373 K from which $\Delta H^{\ominus}$, $\Delta S^{\ominus}$ and $\Delta G^{\ominus}$ (298.15 K) values were obtained, Table 4. The low abundance and small temperature variation of the *E*-dimer signal allowed only an approximate value of $\Delta G^{\ominus}$ (298.15 K) to be calculated for the *E*-dimer–monomer equilibrium.

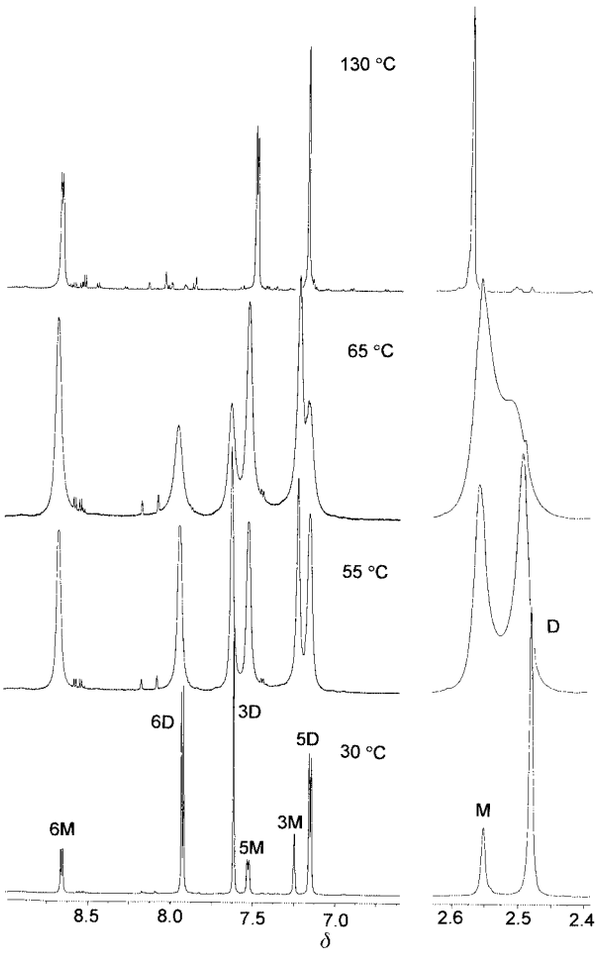

Fig. 3 Variable temperature ^{1}H NMR spectra of 4-methyl-2-nitrosopyridine, **3**, in $(CDCl_2)_2$ solution, showing the effects of dissociation of the *Z*-dimer at above-ambient temperatures.

The solvent and temperature dependencies of the three structural forms of **2** were investigated by NMR studies in $CDCl_3$, CD_2Cl_2, $(CD_3)_2CO$ and $(CD_3)_2SO$ solvents. The results were somewhat inconclusive but the solvent of highest viscosity and relative permittivity, $(CD_3)_2SO$, considerably enhanced the dimer populations. The other solvents affected the equilibria much less. An approximately linear relationship between the dissociation equilibrium constants, $K^{\ominus}$, at a constant temperature, and solvent relative permittivity was found, but the relationship between $K^{\ominus}$ values and solvent viscosity was less clear. The results however do firmly imply that high solvent viscosity/relative permittivity will increase the stability of the azodioxy species, presumably by increasing the rate of monomer association, k_{MZ} or k_{ME}, relative to the rate of dimer dissociation, k_{ZM} or k_{EM}, (see Scheme 1).

Elevation of the solution temperature of **2** favoured dimer dissociation as found for compounds **1** and **3**. This was evident in the ^{1}H NMR spectra of **2** where exchange broadening occurred between the monomer and *Z*- and *E*-dimer signals of the methyl hydrogens and of the 4-, 5- and 6-pyridyl hydrogens with the dimer signals also decreasing considerably in relative intensity. Extraction of reliable rate data by bandshape analysis proved difficult due to small differences of chemical shifts and considerable band overlaps in the regions of interest, coupled with the fact that all monomer signal bandshapes were sensitive to two association rate constants (k_{MZ} and k_{ME}), (Scheme 1). It was anticipated that 2D-exchange spectroscopy (2D-EXSY)[9] would be far better suited to the extraction of reliable rate data, providing temperatures were held below the point at which signals exhibited dynamic broadening. ^{1}H 2D-EXSY spectra of **2** in $CDCl_3$ were therefore measured at three temperatures (303,

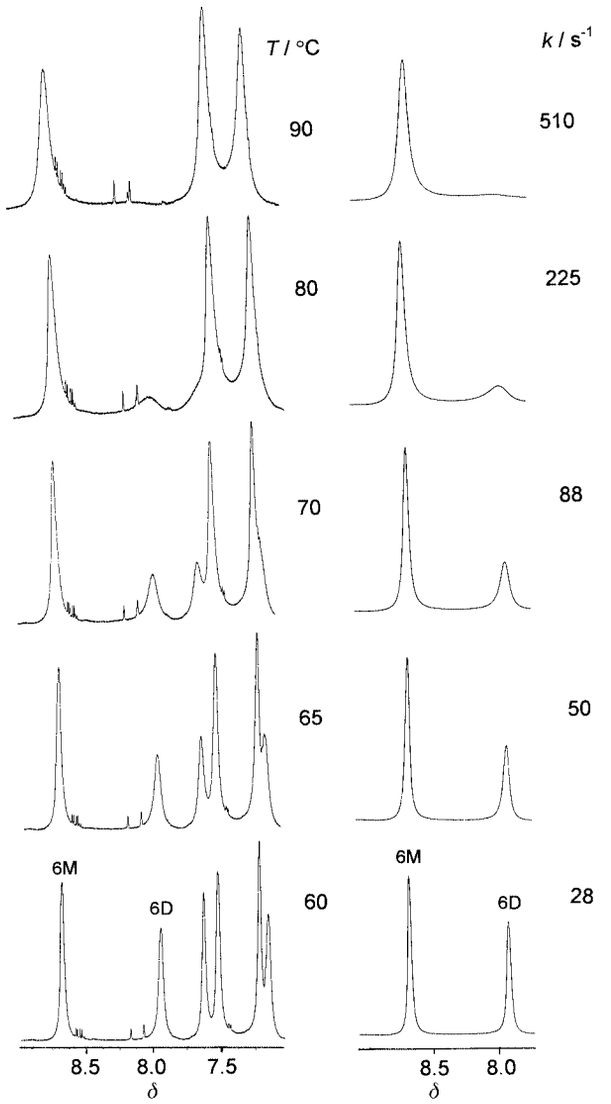

Fig. 4 Bandshape analysis of the 6-position pyridyl monomer (6M) and *Z*-dimer (6D) signals of **3**. The 'best-fit' rate constants shown refer to the D→2M dissociation process.

313 and 323 K) where there was negligible exchange broadening but where the kinetic information could be extracted accurately from the cross peak intensities of the exchanging signals. The aromatic region was chosen for the kinetic analysis and a typical spectrum is shown in Fig. 5. The monomer (M) signals of the 4-, 5- and 6-position hydrogens all show cross peaks with the corresponding *Z*- and *E*-dimer signals (labelled D(*Z*) and D(*E*) respectively). The 6- and 4-position signals produced the clearest, best defined sets of signals, and these were chosen as the basis for the kinetic analysis using the authors' D2DNMR program.[9] Dissociation and association rate constants for the double equilibrium are listed in Table 6. These produced the Eyring activation parameters for **2** included in Table 4.

Compound **2** is the N-heterocyclic analogue of dimeric *o*-nitrosotoluene which was studied extensively by Azoulay *et al.*[21–23] The *Z*-azodioxy dimer of this compound exhibited, at low solution temperatures, hindered rotation about the Ar–N, attributed to the steric interaction of the methyl groups, which, at temperatures below *ca.* −40 °C, led to the detection of two conformers, *Z*,*E* and *Z*,*Z*, which differed in the relationship between the two methyl groups. A similar low temperature study was performed on **2** in CD_2Cl_2 solvent, but no comparable 'freezing out' of conformational isomers was detected at temperatures down to *ca.* −90 °C. Rationalisation of this is reserved for the Discussion below.

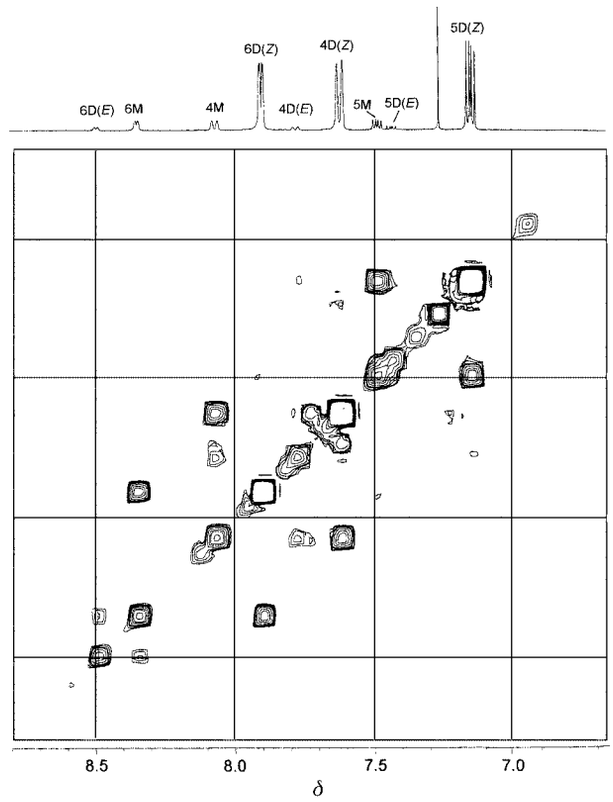

Fig. 5 ^{1}H 2D-EXSY NMR spectrum of 3-methyl-2-nitrosopyridine, **2**, in $CDCl_3$ at 313 K. Only the aromatic signals are shown. Mixing time was 0.5 s. Cross peaks between all dimer D(*Z*) and D(*E*) signals and corresponding monomer (M) signals arising from the dimer dissociation are apparent.

Table 6 Association/dissociation rate data for compound **2** in $CDCl_3$ extracted from ^{1}H NMR 2D-EXSY spectra

Temperature/K	Signal	Mixing time/s	k_{MZ}[a]/ s^{-1}	k_{ZM}[b]/ s^{-1}	k_{EM}[c]/ s^{-1}	k_{ME}[d]/ s^{-1}
303	H4	1.0	0.41	0.05	0.12	0.06
313	H4	0.5	0.94	0.13	0.40	0.14
313	H6	0.5	0.71	0.12	0.32	0.08
323	H4	0.2	1.88	0.52	1.04	0.25
323	H6	0.2	1.81	0.34	1.22	0.20

[a] Monomer→*Z*-dimer. [b] *Z*-dimer→monomer. [c] *E*-dimer→monomer. [d] Monomer→*E*-dimer.

Discussion

Solid-state structures of 1–3

Only the crystal structure of **1** was obtained but it is a reasonable assumption that the *Z*-azodioxy structure is preferred for all three compounds. The structural parameters of particular interest, namely the N–N, N–O and C–N bond lengths, the N–N–O and N–N–C bond angles and the C–N–N–C, O–N–N–O, Ar–N_2O_2 and Ar–Ar dihedral angles, are listed in Table 7 alongside the data for the *Z*-dimers of nitrosobenzene,[19] perfluoronitrosobenzene[20] and 2-nitrosoquinoxaline.[5] X-Ray data are also available for a number of compounds where the *Z*-azodioxy group is incorporated in four-, five- and six-membered rings. These are not genuine $(RNO)_2$ dimers but '*Z*-fixed' N_2O_2 species. There are seven such examples in the literature,[24–28] but their reported N–N, N–O and C–N bond lengths are more variable as they reflect different degrees of ring strain.

The data for the genuine $(RNO)_2$ dimers (Table 7) display a remarkable degree of constancy, ranges of bond lengths being N–N 1.32–1.33 Å, N–O 1.26–1.27 Å and C–N 1.44–1.47 Å.

Table 7 X-Ray crystallographic data for *Z*-azodioxy dimers of related N heteroaromatic compounds

Parameter[a]	**1**[b]	$(C_6H_5NO)_2$[c]	$(C_6F_5NO)_2$[d]	$(C_8H_5N_2NO)_2$[e]
N–N	1.325(3)	1.321(5)	1.324(5)	1.328(6)
N–O	1.260(4)	1.268(4)	1.267(5)	1.259(6)
	1.274(3)			1.264(6)
C–N	1.444(3)	1.454(5)	1.439(6)	1.461(7)
	1.468(4)			
N–N–O	118.1(3)	119.5(2)	119.4(4)	119.3(0.9)
	119.6(2)	120.0(2)		119.6(0.9)
N–N–C	120.4(3)	118.7(2)	119.8(4)	?
	122.5(2)	119.7(2)	120.0(4)	
C–N–N–C	25.80(0.5)	18.0	7.5	11.05
O–N–N–O	4.27(0.4)	3.9	2.4	5.04
Ar–N_2O_2	35.68	64.2	73.4	?
	123.27	112.0	106.1	
Ar–Ar	62.72	62.8	71.2	

[a] Bond angles in Å, bond/dihedral angles in °. [b] Present work. [c] Ref. 19. [d] Ref. 20. [e] Ref. 5.

These near-constant values imply no correlation with ease of dissociation to monomers in organic solvents, as was indeed found for *E*-dimers.[29] This is surprising as the dissociation tendencies of these *Z*-dimers vary considerably. For example, at ambient solution temperatures nitrosobenzene[19] and perfluoronitrosobenzene[20] are 100% monomeric, 2-nitrosoquinoxaline[5] is predominantly monomeric whereas the present 2-nitrosopyridines are predominantly *Z*-dimeric. The presence of a heterocyclic N atom *ortho* to the nitroso function clearly stabilises the *Z*-dimeric form, but the reason for this is unclear. It is notable, however, that the *Z*-dimer of **1** differs considerably from its benzene and perfluorobenzene counterparts in the dihedral angles between the aromatic rings, *viz*. 35.68° compared to 64.2° $(C_6H_5NO)_2$ and 73.4° $(C_6F_5NO)_2$. This results in the two pyridyl rings pointing much more closely towards each other, compared to the other two compounds, with the two heterocyclic N atoms being in close proximity (N···N 2.964 Å). This non-bonded N···N interaction reflects the smaller steric requirements of N compared to C–H and appears to be of overriding importance in conferring stability on the solid state and dominant solution structure of **1**. The smaller degree of twist of the pyridyl rings with respect to the N_2O_2 best-plane will lead to a higher degree of conjugation between the two halves of the dimer. The resulting resonance stabilisation may account for the higher solid-state stability and lower dissociation tendency in solution of the dimeric structure $(C_6H_4NNO)_2$ compared to $(C_6H_5NO)_2$ and $(C_6F_5NO)_2$.

No dihedral angle data have been reported for 2-nitrosoquinoxaline[5] but inspection of a stereoscopic view of the structure indicates a dihedral angle between the two fused-ring planes which is intermediate between that between the pyridyl rings in **1** and that between the phenyl rings in nitrosobenzene, which might account for the moderate dissociation tendency of the quinoxaline compound.

Solution-state structures of 1–3

The present N-heterocyclic *C*-nitroso compounds are distinctive in that their *Z*-dimeric structures are much more stable than their homocyclic counterparts. Indeed their dimeric stabilities are comparable to those of aliphatic *C*-nitroso compounds.[30] Relative dimer/monomer stabilities are reflected in the dissociation equilibrium constants, $K^{\ominus}$, and the thermodynamic data $\Delta H^{\ominus}$, $\Delta S^{\ominus}$, and $\Delta G^{\ominus}$ (298.15 K), Tables 3 and 4. $\Delta H^{\ominus}$ values for these dissociation equilibria are positive and in the range 53–58 kJ mol^{-1}, $\Delta S^{\ominus}$ values are large and positive in the range 154–166 J K^{-1} mol^{-1} and $\Delta G^{\ominus}$ (298.15 K) values are small and positive in the range 4.5–12 kJ mol^{-1}. The latter values imply that, at 298.15 K, the *Z*-dimer forms are thermodynamically favoured, which is in accordance with observations. This is in contrast to nitrosobenzene[19] and its derivatives[31] where negative $\Delta G^{\ominus}$ values imply that dissociation of both *Z*- and *E*-dimers is thermodynamically favoured, as indeed occurs in organic solvents at room temperature.

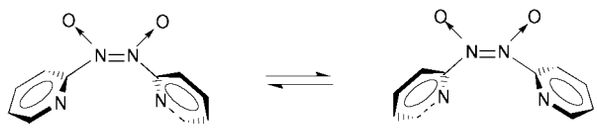

Fig. 6 Proposed solution conformers of **1**, showing torsional oscillation about the pairs of C–N bonds.

In the case of 3-methyl-2-nitrosopyridine, **2**, the *E*-dimer is also present in solution, presumably as a result of the strong steric interactions between the 3-methyl groups and the adjacent N→O functions in the *Z*-dimer. These interactions will be relieved in the *E*-dimer where the pyridyl rings have no preferential orientation with respect to each other and can freely rotate out of the N_2O_2 plane. The negative value of $\Delta G^{\ominus}$ for the *E*-dimer dissociation (Table 4) does however indicate that it is thermodynamically disfavoured compared to the monomer structure at 298.15 K.

The activation energy data for the dimer dissociation processes are given in Table 4. $\Delta H^{\ddagger}$ values are in the range 85–94 kJ mol^{-1}, and $\Delta G^{\ddagger}$ (298.15 K) values, which are less prone to systematic error, are in the range 70–82 kJ mol^{-1}. $\Delta S^{\ddagger}$ values are positive as expected for dimer dissociation processes where the transition state structures are likely to be less tightly bound than the ground state dimer structures. The activation energies are of comparable magnitude to those of nitrosobenzene[19] and its derivatives[31] implying similar differences in ground state and transition state energies of these structures. Methyl substitution on the ring, particularly at the 3-position, causes a slight raising of the activation energy.

The preferred solution conformations of the *Z*-dimers are not known precisely but are likely to be similar to that of the solid-state structure of **1**, with the pyridyl rings slightly twisted with respect to each other and the N heterocyclic atoms in a *syn* relationship. In solution there is likely to be a C_2 symmetry plane bisecting the N=N bond arising from torsional oscillations about the C–N bonds, Fig. 6. Greater degrees of rotation about these bonds, as occurs in *o*-nitrosotoluene,[23] do not appear to occur, presumably because of the strong preference for the heterocyclic N pairs to adopt a *syn* relationship. In the case of **2**, such a *syn* relationship between the pyridyl rings will hold the 3-methyl groups well away from each other. In the alternative structure where the heterocyclic N pairs are in an *anti* relationship strong interactions would occur between the methyls and the pyridyl hydrogens of the *adjacent* ring. No evidence for such interactions was found following a number of NMR nuclear Overhauser enhancement (NOE) experiments performed, in the difference mode, on **2**. It is therefore concluded that in solution the *Z*-dimer structures undergo rapid torsional twists about the two C–N bonds leading to exchange between the pairs of equivalent conformers depicted in Fig. 6.

Acknowledgements

We thank Hannah Cole and Natasha Diakosavas for help with some of the NMR spectral analyses.

We thank the EPSRC for use of the X-ray crystallographic service when it operated at the University of Wales, Cardiff.

References

1 E. C. Taylor, C.-P. Tseng and J. B. Rampal, *J. Org. Chem.*, 1982, **47**, 552.
2 E. C. Taylor, K. A. Harrison and J. B. Rampal, *J. Org. Chem.*, 1986, **51**, 101.
3 R. E. Banks, R. A. Du Boisson, A. Marraccini, L. Sekhri and A. E. Tipping, *J. Fluorine Chem.*, 1987, **37**, 295.

4 R. G. Pritchard, R. E. Banks, A. E. Tipping and P. Haider, *Acta Crystallogr.*, *Sect. C*, *Cryst. Struct. Commun.*, 1991, **47**, 229.
5 J. Armand, Y. Armand, L. Boulares, M. Philoche-Levisalles and J. Pinson, *Can. J. Chem.*, 1981, **59**, 1711.
6 M. Cameron, B. G. Gowenlock and A. S. F. Boyd, *J. Chem. Soc.*, *Perkin Trans. 2*, 1996, 2271.
7 D. A. Fletcher, B. G. Gowenlock, K. G. Orrell, V. Šik, D. E. Hibbs, M. B. Hursthouse and K. M. Abdul Malik, *J. Chem. Soc.*, *Perkin Trans. 2*, 1997, 721.
8 D. A. Kleier and G. Binsch, Program DNMR3, Quantum Chemistry Program Exchange, Indiana University, USA, 1970.
9 E. W. Abel, T. P. J. Coston, K. G. Orrell, V. Šik and D. Stephenson, *J. Magn. Reson.*, 1986, **70**, 34.
10 A. A. Danopoulos, G. Wilkinson, B. Hussain-Bates and M. B. Hursthouse, *J. Chem. Soc.*, *Dalton Trans.*, 1991, 1855.
11 G. M. Sheldrick, SHELX-86, *Acta Crystallogr.*, *Sect. A*, *Fundam. Crystallogr.*, 1990, **46**, 467.
12 G. M. Sheldrick, SHELX-93 Program for Crystal Structure Refinement, University of Göttingen, Germany, 1993.
13 B. G. Gowenlock and W. Lüttke, *Quart. Rev.*, 1958, **12**, 321.
14 W. Lüttke, *Z. Elektrochem.*, 1957, **61**, 302.
15 W. Lüttke, *Z. Elektrochem.*, 1957, **61**, 976.
16 A. Gruger, N. Le Calvé and J. Fillaux, *Spectrochim. Acta*, *Part A*, 1975, **31**, 595.
17 A. Gruger, N. Le Calvé and J. Fillaux, *Spectrochim. Acta*, *Part A*, 1975, **31**, 581.
18 D. A. Fletcher, B. G. Gowenlock and K. G. Orrell, *J. Chem. Soc.*, *Perkin Trans. 2*, 1997, 2201.
19 D. A. Dieterich, I. C. Paul and D. Y. Curtin, *J. Am. Chem. Soc.*, 1974, **96**, 6372.
20 C. K. Prout, A. Coda, R. A. Forder and B. Kamenor, *Cryst. Struct. Commun.*, 1974, 39.
21 M. Azoulay, T. Drakenberg and G. Wettermark, *Tetrahedron Lett.*, 1974, 2243.
22 M. Azoulay, B. Stymme and G. Wettermark, *Tetrahedron*, 1976, **32**, 2961.
23 M. Azoulay, G. Wettermark and T. Drakenberg, *J. Chem. Soc.*, *Perkin Trans. 2*, 1979, 199.
24 C. K. Prout, V. P. Stothard and D. J. Watkin, *Acta Crystallogr.*, *Sect. B*, *Struct. Crystallogr. Cryst. Chem.*, 1978, **34**, 2602.
25 C. K. Prout, T. S. Cameron, R. M. A. Dunn, O. J. R. Hodder and D. Viterbo, *Acta Crystallogr.*, *Sect. B*, *Struct. Crystallogr. Cryst. Chem.*, 1971, **27**, 1310.
26 F. M. Miao, D. Chantry, T. Harper and D. C. Hodgkin, *Acta Crystallogr.*, *Sect. B*, *Struct. Crystallogr. Cryst. Chem.*, 1982, **38**, 3152.
27 S. N. Whittleton and J. D. Dunitz, *Acta Crystallogr.*, *Sect. B*, *Struct. Crystallogr. Cryst. Chem.*, 1982, **38**, 2052.
28 S. N. Whittleton and J. D. Dunitz, *Acta Crystallogr.*, *Sect. B*, *Struct. Crystallogr. Cryst. Chem.*, 1982, **38**, 2053.
29 B. G. Gowenlock and K. J. McCullough, *J. Chem. Res.* (*S*), 1997, 270.
30 B. G. Gowenlock and J. Trotman, *J. Chem. Soc.*, 1956, 1670.
31 D. A. Fletcher, B. G. Gowenlock and K. G. Orrell, *J. Chem. Soc.*, *Perkin Trans. 2*, 1998, 797.